

Evaluations on Vortex Based Doppler Velocity Dealiasing Algorithm for Tropical Cyclones

Wei-Tin Fang¹, Pao-Liang Chang², Pin-Fang Lin¹

Meteorological Satellite Center¹, Meteorological Information Center²
Central Weather Bureau, Taipei, Taiwan

Abstract

In this study, a vortex-based Doppler velocity dealiasing (VDVD) algorithm with iterative procedures based on the Rankine combined vortex assumption is proposed to improve Doppler velocity quality for tropical cyclone (TC) cases. An idealized case based on the ground-based velocity track display (GBVTD) and GBVTD-simplex techniques shows reasonable results for recovering the aliased velocity and finding the proper TC center. For Typhoon Fitow (2013), which was observed by Wu-Fen-San radar, the proposed vortex-based Doppler velocity dealiasing algorithm recovers most of the aliased velocity observations with 99.4 % accuracy for all pixels, based on 472 data sweeps. For 87 % (95.6 %) of data sweeps, the data success rate is more than 99 % (98 %), compared to that of 70.6 % (79.7 %) for data sweeps when using the Zhang and Wang (2006) (hereafter, ZW06) algorithm. In addition, there is a data success rate of approximately 2 % for sweeps lower than 97 % when using the VDVD algorithm, compared to that of more than 14 % of sweeps when using the ZW06 algorithm. The success rate of the VDVD for each sweep varies from 93.6 to 100 %, and the success rate of the ZW06 algorithm varies from 74.5 to 99.97 %. In addition, it is found that the local circulations generated by terrain would might conflict with the assumption of Rankine combined vortex and result in inadequate dealiased Doppler velocities from VDVD algorithm. Therefore, the radial-by-radial verification procedure is adopted to recover from the consequences caused by local circulations.

Generally, the VDVD algorithm can provide high-quality Doppler velocity for TC cases. Using the VDVD aliased data, a stable performance is observed for the temporal evolution of mean tangential winds based on single radar wind retrievals (GBVTD algorithm). Significant circulation characteristics are also presented in the inner core of a typhoon based on dual Doppler wind retrievals and associated wind composite analyses. It's suggested that the VDVD algorithm can improve the quality of downstream applications such as Doppler wind retrievals and radar data assimilations of TCs and other storms with vortex signatures such as tornadoes and mesocyclones.

Key words: radar, Doppler velocity, Velocity dealiasing, Typhoon, Tropical cyclone

1. Introduction

On average, there are approximately 3-4 typhoons that affect Taiwan per year. To improve the monitoring and prediction of flash floods, debris flows, severe storms and typhoons, a radar network was implemented in Taiwan (Chang et al. 2009). However, an inadequate Doppler velocity dealiasing process would significantly increase the uncertainties of basic interpretations and downstream applications such as single- and dual-Doppler wind retrievals and data assimilations in real-time operations and research. To improve the accuracy of velocity dealiasing for TCs, a vortex-based Doppler velocity dealiasing algorithm is proposed in this study.

2. Methodology

The Doppler velocity is proportional to the Doppler shift and will encounter the aliased problem when the Doppler shifts exceed the maximum detectible phase.

Fundamentally, the observed Doppler velocity V_d and unfolded velocity V_u can be expressed by

$$V_u = V_d \pm 2n \times V_n \quad (1)$$

where n is an integer (0, 1, 2, ..), and V_n represents the Nyquist velocity.

To eliminate the aliasing effects a vortex-based Doppler velocity dealiasing algorithm is proposed by combining the GBVTD (Lee et al. 1999) and GBVTD-simplex (Lee and Marks 2000) techniques and the Rankine combined vortex concept. The GBVTD technique provides an objective approach to estimate the primary TC circulation including the mean flow, axisymmetric tangential and radial winds, and asymmetric tangential winds from single Doppler radar data. Because the GBVTD calculations are on a ring with a constant radius from the TC center, the quality of the GBVTD-retrieved TC circulation strongly depends on an accurate center position. Accordingly, Lee and Marks (2000) proposed an algorithm using the simplex method to objectively estimate the TC vorticity center by

maximizing the GBVTD-retrieved mean tangential wind; this method reduces uncertainties in estimating the TC center position and improves the quality of the GBVTD-retrieved TC circulation (Lee and Marks 2000; Bell and Lee 2002 2012). By combing the GBVTD and GBVTD-simplex techniques and profiles of Rankin-like vortex for TCs, the aliased Doppler velocity can be sequentially dealiased with the iterative procedures. In VDVD algorithm, the radius of the maximum wind and the maximum velocity can be estimated from the GBVTD technique and circulation center can be estimated from GBVTD-simplex technique, all the estimated information then can be applied into Rankin-like vortex to extend that wind model to a larger radius.

3. Sensitivity Tests

An idealized Rankine combined vortex is used for the sensitivity tests. Two tests are performed: one test is GBVTD based on the unfolding algorithm, and the other test is GBVTD and GBVTD-simplex based on the unfolding algorithm. The idealized vortex is given as $V_{max} = 70 \text{ m s}^{-1}$, $R_{max} = 60 \text{ km}$, and $\alpha = 0.5$ at 23.91°N and 122.26°E , as shown in Figure 1a. The radar Nyquist velocity (V_n) is set to 33.6 m s^{-1} for the radar observations.

To test the performance of the initial estimates of V_{guess} and R_{guess} for the initial reference vortex, a V_{guess} of $0\text{-}130 \text{ m s}^{-1}$ and R_{guess} of $0\text{-}130 \text{ km}$ are used to approach the V_{max} and R_{max} . The differences between the V_{guess} and R_{guess} values and GBVTD-derived V_{max} and R_{max} (dV and dR) values are also calculated. Figure 2a shows the convergent feature diagram where the vector and amounts of change are from the dVs and dRs calculated at V_{guess} and R_{guess} . Nearly all vectors are indicating toward the points at $V_{max} = 70 \text{ m s}^{-1}$ and $R_{max} = 60 \text{ km}$ (Fig. 2a). This finding also reveals that most combinations of V_{guess} and R_{guess} are suitable for an initial estimate, except the combination of a high V_{guess} and low R_{guess} . The high V_{guess} and low R_{guess} result in an irreversible unfolding process, which incorrectly drives two velocity dipoles similar to those from the double eyewall (Fig 2b). Therefore, a lower V_{guess} with a wide range of V_{guess} is relatively adequate for retrieving the vortex structure with the GBVTD-based unfolding algorithm. A simple test with $V_{guess} = 33.6 \text{ m s}^{-1}$, $R_{guess} = 30 \text{ km}$ and GBVTD-retrieved results for every individual iteration are shown in Table 1 and plotted in Figure 1 as Rankine profiles. In the initial iteration, even the reference vortex is far from the idealized vortex and results in an incorrect unfolded velocity field near the eyewall. The V_{max} and R_{max} values derived from the GBVTD algorithm are 55.76 m s^{-1} and 48 km , which are both closer to the given values of the idealized vortex ($V_{max} = 70 \text{ m s}^{-1}$, $R_{max} = 60 \text{ km}$) than are those initially estimated ($V_{guess} = 33.6 \text{ m s}^{-1}$, $R_{guess} = 30 \text{ km}$). The differences in V_{max} (dV) and R_{max} (dR) are 22.16 m s^{-1} and 18 km , respectively. In the second iteration, the GBVTD-derived V_{max} and R_{max} values are 70.06 m s^{-1} and 61 km , which are very close to the idealized vortex values. In the third iteration, there are no differences in the V_{max} and R_{max} values between the third initial estimate and the GBVTD-derived value, and thus stop the iterations. With this

idealized vortex, the simulated aliasing Doppler velocity can be correctly dealiased with only 3 iterations, indicating that the scheme is highly computationally efficient in the iterations.

To investigate the impact of different TC centers on the GBVTD-derived V_{max} , TC centers within 23.25°N to 24.25°N and 121.86°E to 127.36°E are simulated. Additionally, the GBVTD-simplex algorithm was applied to find the TC center. Figure 2a shows the GBVTD-derived V_{max} distribution, which indicates that the area with a V_{max} greater than 60 m s^{-1} occupied nearly the entire northwestern quadrant of the first estimation. Figure 2a also shows the exact center (black solid typhoon symbol) that can be efficiently determined by following the procedures described in Lee and Marks (2000). However, the wrong center might result in an asymmetric structure when the vortex center is too far from the actual center. In this situation, the pattern of V_{max} (wave number 0) distribution would change from circular to elliptical shape and the amplitude of wave numbers 1 and 2 should be simultaneously amplified. To mitigate this effect, the V_{max} is calculated as wave number 0 minus the summation of wave numbers 1 and 2. Figure 2b shows a more concentrated local maximum pattern of V_{max} after the modification that significantly improved the GBVTD-simplex algorithm performance.

4. Results and Evaluations

Two typhoon cases with and without landfall on Taiwan were used to investigate the VDVD algorithm success rates. One case was Typhoon Fitow (2013), which passed over the ocean northeast from Taiwan with the typhoon center more than 100 km away from the northern tip of Taiwan. The other case was Typhoon Nesat (2017), which exhibited a westerly track similar to Typhoon Fitow. However, Nesat's track was further south and made landfall on the northeastern Taiwan.

a. Typhoon Fitow (2013)

Figure 3 show the extreme examples of ZW06 Typhoon Fitow (2013). The center of Typhoon Fitow locates over the ocean northeast from Taiwan with a distance of $\sim 240 \text{ km}$ to the radar site at 2311 UTC 5 Oct 2013. It exhibited a weakly circular-symmetric eyewall structure with a radius of $\sim 50 \text{ km}$ and weak echo areas existing in the eye region (Fig. 3a). Because of the high wind speed from typhoon Fitow, it is obvious that the raw Doppler velocities observed by RCWF radar are unreasonable in the outer eyewall area (Fig. 3b). The Doppler velocities which apply ZW06 algorithm is presented in Figure 3c. It is the worst case of the ZW06 algorithm only has a success rate of 74.5% compared with the subjective dealiasing analysis. Some unreasonable Doppler velocities were seen near the northwestern to southwestern quadrants of the TC center, which occasionally occurred during operation due to relatively noisy data around the eyewall areas (Fig. 3e). In contrast, VDVD algorithm has a success rate more than 99% at this time (Fig. 3e). After reviewing the whole results from VDVD algorithm, it is found that the performance is very

well for Typhoon Fitow except for the cases that are affected by sea clutter and the worst successful rate is 93.6%.

b. Typhoon Nesat (2017)

Figure 4a shows the reflectivity field of Typhoon Nesat observed from RCHL at 0922 UTC 29 July. It is found that the obvious asymmetric eyewall structure with strong reflectivity locating in southern quadrant of typhoon center. The center is located about 75 km northeast of radar site with an eyewall radius of ~ 50 km. Because Typhoon Nesat (2017) is close to the east coast line of Taiwan at this time, the aliased Doppler velocity does not only occur over eyewall and surrounding area but also occurs over the area near the offshore areas of southeastern Taiwan due to local circulation generated by terrain (Fig. 4b). Figure 4c is the VDVD results and shows that the aliased velocities can be recover over eyewall and surrounding area. However, there are some discontinuities in the Doppler velocities that are overly dealiased near the offshore areas of southeastern Taiwan with the typhoon circulation velocity profiles, which frequently deviate from the Rankine combined vortex assumption due to the terrain-generated local circulations. As a result, the basic assumption of the VDVD algorithm cannot be adequately applied because of the local circulations. To avoid this situation and extend the VDVD algorithm usage, a procedure of radial-by-radial verification similar to the beam checking in ZW06 is used to recover the discontinuities resulting from inadequate unfolding. Figure 4d shows the dealiasing velocity field from VDVD algorithm to which the radial-by-radial verification procedure is appended. The discontinuous areas are significantly reduced, indicating that the radial-by-radial verification procedures can recover the inadequately dealiased Doppler velocities, once the local circulations outside the TC inner core areas are far from the Rankine combined profile assumption.

5. Application Performance of Wind Retrievals

To further evaluate the application performance of the VDVD algorithm, the retrieved wind of the GBVTD and dual Doppler wind synthetic techniques are used to investigate the difference of retrieved wind between that applying the ZW06 and VDVD algorithm.

a. GBVTD retrievals

Figure 5 shows comparisons of the temporal evolution of the mean tangential winds derived from the GBVTD, based on the dealiasing data of the ZW06 and VDVD algorithms from the RCHL radar for Typhoon Nesat (2017). The RMW exhibits a decreasing trend prior to landfall and presents a very evident RMW contraction from 50 km to 25 km (0807 to 1100 UTC) before Typhoon Nesat made landfall on Taiwan, based on the VDVD dealiased data observed from the RCWF radar. The RMW contraction rate is 25 km 3h⁻¹ (Fig. 5a). In contrast, using the ZW06 dealiased data, the extremely discontinuous gaps in the spatial and temporal distributions of the mean

tangential wind indicated that a large area of data were not adequately dealiased.

b. Dual Doppler wind retrievals

To analyze the overall characteristics of the inner core region, the 2D mosaic winds are composited, as the lowest available data are collected from all dual Doppler retrieval winds at every analysis elevation similar to the hybrid reflectivity. Generally, the inner core region of Typhoon Nesat (2017) exhibits an approximately circular circulation, with the maximum wind occurring in the southeastern quadrant of the eyewall, based on the VDVD aliased data (Fig. 6a). In addition, the RMW is close to 50 km with a maximum wind speed of more than 55 m s⁻¹ from altitudes 2-3 km located near northeastern quadrant of inner side of eyewall. The unreasonable retrieval wind in the northern and northeastern quadrants is obvious when using ZW06 data (Fig. 6b), indicating that the inadequate dealiasing of Doppler velocity potentially contaminates the results of downstream analyses at all altitudes.

6. Conclusions

In this study, a VDVD algorithm with iterative procedures based on the Rankine combined vortex assumption is proposed to improve Doppler velocity quality for typhoon cases. A sensitivity test for an idealized case based on GBVTD and GBVTD-simplex technique shows reasonable results for the recovery of the aliased velocity and the determination of a proper TC center. A set of quality control procedures is also applied to the real cases. The Doppler velocity of Typhoon Fitow (2013) observed by the Wu-Fen-San radar is used to evaluate the performance of the VDVD algorithm. The VDVD algorithms recovered most of the aliased velocity observations with a 99.4 % accuracy of all pixels based on 472 data sweeps. Eighty-seven percent (95.6 %) of sweeps show data success rates of more than 99 % (98 %), compared to that of 70.6 % (79.7 %) of sweeps for the ZW06 algorithm. In addition, only 2 % of data sweeps show a success rate of lower than 97 % for the VDVD algorithm, compared to that of more than 14 % of sweeps for the ZW06 algorithm. The success rate of the VDVD algorithm for each sweep varies from 93.6 to 100 %, and the success rate of the ZW06 algorithm varies from 74.5 to 99.97 %. The unsuccessful pixels mainly result from the influence of sea clutters that are frequently embedded with weather echoes and reduce the success rate of the VDVD algorithm. Hence, sea and other clutters should be adequately removed in advance to further improve the VDVD algorithm performance. In the case study of Typhoon Nesat (2013), radial-by-radial verification procedures can recover the inadequately dealiased Doppler velocities, even when local circulations outside the inner core areas of TCs are far from the Rankine combined profile assumption.

Generally, the VDVD algorithm can provide a high-quality Doppler velocity for TCs to improve the quality of downstream analyses. This algorithm shows a better performance than the ZW06 algorithm when it is applied

to single and dual Doppler wind retrievals. The VDVD dealiased data shows a reasonable temporal evolution of the mean tangential winds from single radar wind retrievals using the GBVTD algorithm compared to a discontinuous one using ZW06 algorithm. The VDVD algorithm also shows significant circulation characteristics in the inner core of the typhoon using dual Doppler wind retrievals and their associated wind composite analyses.

For further performance evaluation and improvement, typhoon cases with different tracks and strengths near Taiwan will be examined in the future. Subsequently, the VDVD algorithm will be applied to real-time operations to improve the quality of Doppler velocity for downstream applications, such as Doppler wind retrievals and radar data assimilations of TCs and storms with vortex signatures such as tornadoes and mesocyclones.

References

- Chang, P. -L., B. J.-D. Jou, and J. Zhang, 2009: An algorithm for tracking eyes of tropical cyclones. *Wea. Forecasting*, **24**, 245–261.
- Lee, W. -C., B. J. -D. Jou, P. -L. Chang, and S. -M. Deng, 1999: Tropical cyclone kinematic structure retrieved from single-Doppler radar observations. Part I: Interpretation of Doppler velocity patterns and the GBVTD technique. *Mon. Wea. Rev.*, **127**, 2419–2439.
- Lee, W.-C., and F. D. Marks Jr., 2000: Tropical cyclone kinematic structure retrieved from single-Doppler radar observations. Part II: The GBVTD-simplex center finding algorithm. *Mon. Wea. Rev.*, **128**, 1925–1936.
- Bell, M. M., and W.-C. Lee, 2002: An objective method to select a consistent set of tropical cyclone circulation centers derived from the GBVTD-simplex algorithm. Preprints, *25th Conf. on Hurricanes and Tropical Meteorology*, San Diego, CA, Amer. Meteor. Soc., 642–643.
- Bell, M. M., and W. Lee, 2012: Objective tropical cyclone center tracking using single-Doppler radar. *J. Appl. Meteor. Climatol.*, **51**, 878–896.
- Zhang, J., and S. Wang, 2006: An automated 2D multipass Doppler radar dealiasing scheme. *J. Atmos. Oceanic Technol.*, **23**, 1239–1248.

Table 1. GBVTD derived V_{max} and R_{max} in each iteration

iteration	V_{guess}	R_{guess}	V_{GBVTD}	R_{GBVTD}
0	33.60	30	56.80	49
1	56.80	49	70.06	61
2	70.06	61	70.07	61

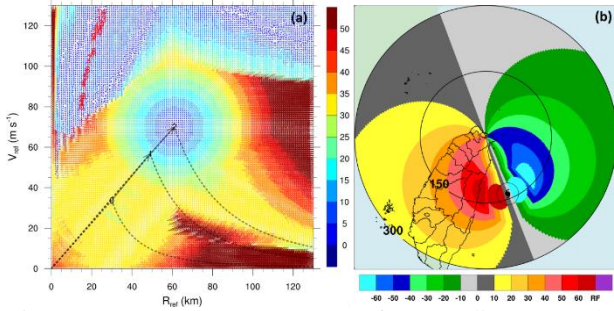


Figure 1. (a) The convergent feature diagram. The numbers and arrows with black are the iteration number and path, as seen in Table 1. The Rankine combined wind profiles used in consecutive iteration are indicated with dash lines. The red text and line on the upper left indicate the iteration number and path based on an improper initial estimate. The color scale indicates the square root of summation from the R_{max} and V_{max} differences between the estimate and true value during the calculations (see text for detail). (b) The dealiasing results of the Doppler velocity correspond to the improper initial estimate in (a). The color scale indicates the Doppler velocity, and the gray circle centered on the typhoon symbol indicates the maximum wind radius.

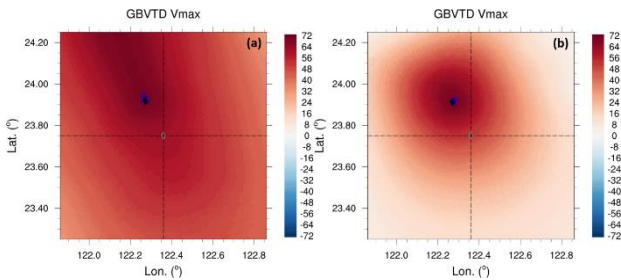


Figure 2. The V_{max} distribution of (a) GBVTD-simplex and (b) GBVTD-simplex with an adjustment in V_{max} . The typhoon symbol with gray is the original initial guess of TC position. Blue numbers indicate the results of GBVTD-simplex from 16 initial guesses by adding small disturbances to original initial position (gray typhoon symbol). Typhoon symbol with black is the final result determined from 16 initial guesses.

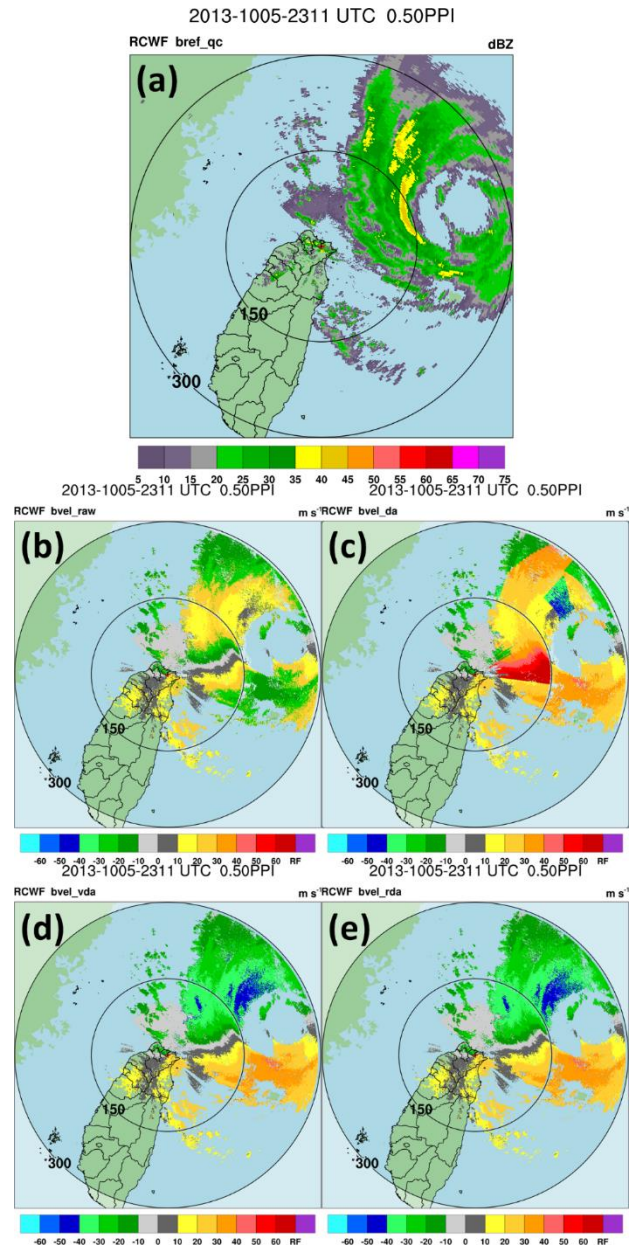


Figure 3. Radar observations of Typhoon Fitow (2013) at 0.5 degrees from RCWF at 2311 UTC 5 Oct 2013. (a) Base reflectivity. Doppler velocity of (b) raw data, (c) Zhang and Wang (2006), (d) VDVD, and (e) subjective analysis.

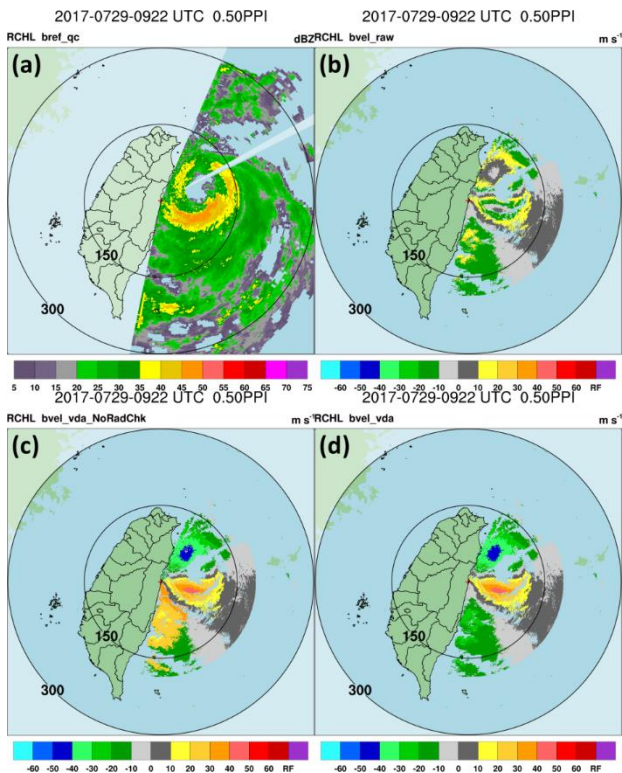


Figure 4. Radar observations of Typhoon Nesat (2017) at 0.5 degrees from RCHL at 0922 UTC 29 July 2017. (a) Base reflectivity. Doppler velocity of (b) raw data, (c) VDVD, and (e) VDVD with radial verification procedure.

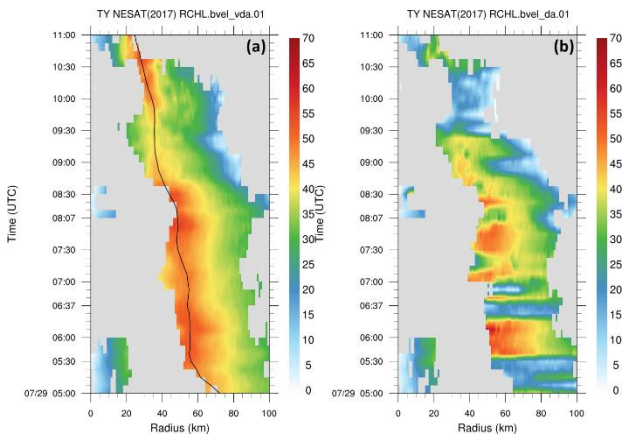


Figure 5. (a) A temporal composite of the Nesat mean tangential wind (m s^{-1}) derived with the GBVTD technique using VDVD dealiased data from the RCHL radar between 0500 and 1100 UTC 29 Jul 2017. Shading intervals are every 5 m s^{-1} , and the solid lines indicate the RMW. (b) Same as in (a) but with ZW06 dealiased data.

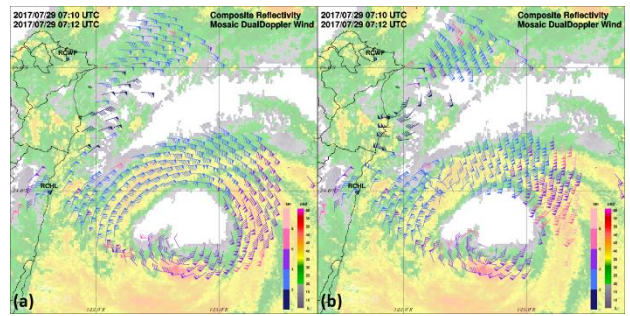


Figure 6. Composite dual Doppler wind retrievals from Typhoon Nesat at 0712 UTC on 29 July 2017 retrieved from the RCWF and RCHL radars using (a) VDVD and (b) ZW06 dealiased data. The wind bars in dark blue, blue, purple, red pink and pink indicate wind retrievals from levels of 0–2, 2–4, 4–6, 6–8 and above 8 km, respectively.

